A continuum damage mechanics model with the strain-based approach to biaxial low cycle fatigue failure

A. Zolochevsky, T. Itoh, Y. Obataya, J. Betten

Abstract A continuum damage mechanics model for low cycle fatigue failure of initially isotropic materials under biaxial loading conditions is presented. The expression for the equivalent strain in the fatigue damage evolution equation contains the three material parameters, and the strain intensity as well as the maximum principal strain and the volume strain for amplitudes. It is shown how these material parameters can be determined from a series of basic experiments using a cruciform specimen. Particular expressions for the equivalent strain with a smaller number of material parameters and invariants are obtained. Model predictions are found to be in satisfactory agreement with the experimental low cycle fatigue data under full ranged biaxial loadings obtained in the test using a cruciform specimen.

Ein mechanisches Kontinuumsschadenmodell mit einem Ansatz, der auf Spannungen basiert, für Bruch wegen zweiachsiger zyklischer Ermüdung.

Zusammenfassung Ein mechanisches Kontinuumsschadenmodell für Bruch wegen zweiachsiger zyklischer Ermüdung von ursprünglich isotropen Materialien unter zweiachsigen Belastungsbedingungen wird dargestellt. Der Ausdruck für die äquivalente Spannung in den Gleichungen für die Entwicklung des Ermüdungsschadens beinhaltet 3 Materialparameter, die Amplituden der Spannungsintensität, der maximalen Hauptspannung und die der Volumenspannung. Es wird gezeigt, wie diese Materialparameter mittels einer Reihe grundlegender Experimente an kreuzförmigen Probekörpern bestimmt werden können. Besondere Ausdrücke für die äquivalente Spannung mit einer geringeren Anzahl von Materialparametern und Invarianten resultieren. Modellvorhersagen stehen in befriedigender Übereinstimmung mit den experimentellen Ermüdungsdaten nach wenigen Zyklen unter im ganzen Bereich von zweiachsigen Belastungen. Für diese Testexperimente wurden kreuzförmige Probekörper benutzt.

List of symbols

A, B, C	Material constants
a, b, d, r, f, m, k	Material parameters
N	Number of cycles
N_*	Number of cycles to failure
ϕ	Principal strain ratio
ε_{kl}	Components of the strain tensor for amplitudes
e_{kl}	Components of the strain deviator for amplitudes
α , γ	Numerical coefficients
δ_{kl}	Kronecker's delta
λ_1 , λ_2 , λ_3	Material parameters
ε_e	Equivalent strain
ε_i	Strain intensity for amplitudes
ε_0	Volume strain for amplitudes
$\varepsilon_{11}, \varepsilon_{22}, \varepsilon_{33}$	Amplitudes of the principal strains
$\chi(\varepsilon_e)$	Some function of the equivalent strain
ω	Damage variable
ν	Poisson's ratio

1 Introduction

A comprehensive review of low cycle fatigue damage models for polycrystalline materials has been given by Fatemi and Yang [1]. Existing multiaxial low cycle fatigue damage theories can be divided into three groups. They are stress-based [2-5], strain-based [2,6-8] and energy-based [3,9-11] models. However, these fatigue damage theories were developed under the limited multiaxial stress/strain states.

Multiaxiality of loading affects on low cycle fatigue lives of materials largely. The features of this influence may be investigated experimentally. In this way, a large number of tests on laboratory specimens have been performed in realistic environmental conditions. Therefore, different types of laboratory specimens may be used to vary the degree of multiaxiality, such as hollow cylindrical specimens under combined tension and torsion [2,7-9,12-14], an annular disk specimen with a reduced testing section [10], thin-walled tubes under tension and internal/external pressure [15-17], cruciform specimens [11,18-22], notched cylindrical specimens [23,24], etc.

The aim of this paper is to propose a new continuum damage mechanics model based on the equivalent strain concept for evaluating the damage growth and fatigue life under biaxial loading conditions for initially isotropic polycrystalline materials. We will use the results of strain controlled biaxial low cycle fatigue tests obtained on the basis of cruciform specimens [20,21]. These experimental results shown in Fig.1 clearly demonstrate the effect of the amplitude of the maximum principal strain as well as the strain biaxiality which is defined by the

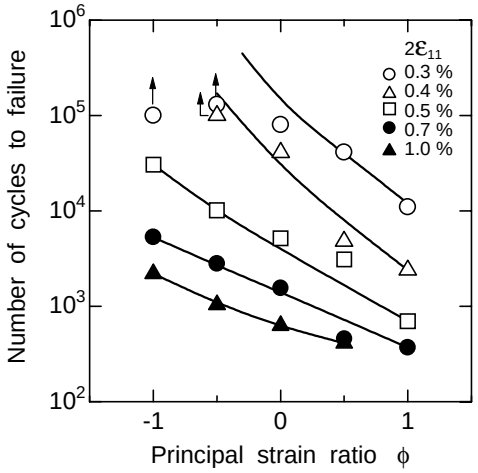

Fig.1. Relationship between biaxial fatigue life and principal strain ratio

principal strain ratio $\phi=\varepsilon_{22}/\varepsilon_{11}$ on biaxial low cycle fatigue lives for type SUS304 stainless steel at 923K [20,21]. Here, ε_{11} and ε_{22} are the maximum and minimum principal strains in the plane of cruciform specimen surface. Testing machine on the basis of cruciform specimens can perform biaxial low cycle fatigue tests in the range of $-1\le\phi\le1$, which is full range of biaxial strain state under plane stress condition.

2 Continuum damage mechanics model

A number of comments need to be made. Firstly, equivalent strain concept gives an opportunity to relate all fatigue endurance data under multiaxial loading to corresponding primary fatigue endurance data from simple tests (basic experiments). Secondly, an approach based on the strain intensity introduced and used in classical theory of plasticity and on one material parameter which can be found from the one type basic experiments is not applicable to describe the fatigue behavior for many materials [2,8,10,18,22,23]. Thirdly, Nurtjahjo *et al.* [19] made a conclusion on the basis of biaxial experiments on cruciform specimens that a number of one parameter approaches as well as the two parameter approach proposed by Brown and Miller [6] can not reproduce the actual biaxial fatigue behavior of the Al7475-T7351 material.

In the following, we shall use the basic aspects of continuum damage mechanics based on the original concepts of Kachanov [25] and Rabotnov [26]. The fundamental aspects of continuum damage mechanics can be found in references [27-33].

In order to describe fatigue damage accumulation per cycle, we introduce the damage variable $\omega\in[0, 1]$ which may be defined according to Rabotnov [28] as the microcrack area density or net area reduction in the observed plane. The damage variable is a function of number of cycles, i.e. $\omega=\omega(N)$. An initial value $\omega=0$ corresponds to the undamaged state for $N=0$, while a critical value $\omega=1$ corresponds to fatigue failure for number of cycles to failure $N=N_*$. It is possible to describe the damage growth by the following fatigue damage evolution equation [4,5,28]:

$$\frac{d\omega}{dN}=(1-\omega)^{1-k}\chi(\varepsilon_e) \tag{1}$$

where ε_e is the equivalent strain, k is material parameter, exponent "1-k" is taken in order to receive the simple formula in the following. The function $\chi(\varepsilon_e)$ in Eq.(1) may be determined through the experimental data related the strain amplitudes to the number of cycles to failure in basic experiments. This function may be written in one of the following form: the power relation $\chi(\varepsilon_e)=\varepsilon_e^r$, the hyperbolic sine law $\chi(\varepsilon_e)=\sinh(\varepsilon_e/d)$ or exponential relation law $\chi(\varepsilon_e)=\exp(\varepsilon_e/f)$. In order to describe the fatigue behavior, when the equivalent strain varies in the interval $\varepsilon_e\in(a,\ b)$, it is conveniently to use the following formula:

$$\chi(\varepsilon_e)=\left(\frac{\varepsilon_e-a}{b-\varepsilon_e}\right)^m \tag{2}$$

Here r, d, f, a, b and m are material parameters.

We shall consider in-plane symmetrical cyclic loading. In this case the equivalent strain can be introduced as:

$$\varepsilon_e=\lambda_1\varepsilon_i+\alpha\lambda_2\varepsilon_{11}+\gamma\lambda_3\varepsilon_0 \tag{3}$$

where λ_1, λ_2 and λ_3 are material parameters, α and γ are numerical coefficients which take into account the specific weight for different terms in Eq.(3). ε_i and ε_0 in Eq. (3) are the strain intensity and the volume strain for the amplitudes, respectively, which are defined as:

$$\varepsilon_i=\sqrt{\frac{2}{3}e_{kl}e_{kl}},\quad \varepsilon_0=\varepsilon_{kl}\delta_{kl} \tag{4}$$

where

$$e_{kl}=\varepsilon_{kl}-\frac{1}{3}(\varepsilon_{mn}\delta_{mn})\delta_{kl} \tag{5}$$

are components of the strain deviator for the amplitudes, δ_{kl} is the Kronecker's delta.

It is seen that the equivalent strain given by Eq.(3) is assumed to consist of three terms. The first term reflects the influence of movement of dislocations and slipping on the fatigue damage growth. The last two terms in the expression for the equivalent strain reproduce the influence of the maximum principal strain and the volume strain on the fatigue damage. If these invariants have no influence on the fatigue damage growth, then we must put $\alpha=\gamma=0$ in Eq.(3). Obviously, numerical coefficients α and γ reflect the influence of the maximum principal strain and the volume strain, respectively, on the damage development.

In the case of constant amplitude loading, the number of cycles to failure can be obtained by integrating Eq.(1), and is equated as

$$N_* = \frac{1}{k\chi(\varepsilon_e)} \tag{6}$$

3 Basic experiments

We now consider a procedure for the determination of three parameters λ_1, $\alpha\lambda_2$ and $\gamma\lambda_3$ in Eqs (2), (3) and (6) for the case of constant amplitude loading which needs the results of the basic experiments on cruciform specimens. Let the Cartesian coordinate axes 1 and 2 are located in the plane of the specimen surface. Then the axis 3 will be to coincide with the normal direction to this plane. We recall that ε_{11} and ε_{22} are the amplitudes of the maximum and minimum principal strains in the plane of the specimen surface, respectively, i.e. $\varepsilon_{11}\geq\varepsilon_{22}$, and $\phi=\varepsilon_{22}/\varepsilon_{11}$ is the principal strain ratio.

A number of comments need to be made. Firstly, the experimental determination of the strain ε_{33} presents greater technical difficulties while comparing the strains ε_{11} and ε_{22}. Secondly, due to the technical impossibility to experimentally determine the strain ε_{33} using a biaxial fatigue testing machine, many authors [18-22] assume the condition of incompressibility, i.e.

$$\varepsilon_{33} = -(\varepsilon_{11} + \varepsilon_{22}) \tag{7}$$

In other words, they assume that in low cycle fatigue the Poisson's ratio

$$\nu = 0.5 \tag{8}$$

However, applicability of Eqs (7) and (8) for practical problems is very questionable. For example, even under the condition (7) number of cycles to failure for the 316FR steel in case with $\phi=-1$ is more than 7 times as high as the analogous magnitude in the case with $\phi=0$ for one and the same value of strain intensity $\varepsilon_i=10^{-3}$ calculated on the basis of Eqs (4), (5) and (7) [22]. Thirdly, the expression (3) for the equivalent strain together with Eq. (4) can be rewritten for the case under consideration in the following form

$$\varepsilon_e = \frac{\sqrt{2}}{3}\lambda_1\sqrt{(\varepsilon_{11}-\varepsilon_{22})^2+(\varepsilon_{11}-\varepsilon_{33})^2+(\varepsilon_{22}-\varepsilon_{33})^2} + \alpha\lambda_2\varepsilon_{11} + \gamma\lambda_3\varepsilon_0 \tag{9}$$

Then we note that in contrast to the strain ε_{33}, the strains ε_{11} and ε_{22} can be controlled independently and with necessary accuracy. Furthermore, we have no information about the effect of the strain ε_{33} on the fatigue life of cruciform specimen. Therefore, we can assume that the strain ε_{33} has much smaller effect on the fatigue damage accumulation while comparing the strains ε_{11} and ε_{22}. In this regard, we arrive at the assumption that

$$\varepsilon_{33} \cong 0 \tag{10}$$

in the expression (9) for the equivalent strain. Thus, in the following we can use the equivalent strain given by Eq. (3) together with the following expressions for the strain intensity and the volume strain

$$\varepsilon_i = \frac{2}{3}\sqrt{\varepsilon_{11}^2 - \varepsilon_{11}\varepsilon_{22} + \varepsilon_{22}^2}, \quad \varepsilon_0 = \varepsilon_{11} + \varepsilon_{22} \tag{11}$$

We shall later show that assumption (10) gives the opportunity to predict satisfactory biaxial fatigue lives.

Considering basic experiments on cruciform specimens, we obtain for each principal strain ratio ϕ such relations between the number of cycles to failure and the amplitude of maximum principal strain as:

$$N_* = \frac{1}{k\left(\frac{A\varepsilon_{11}-a}{b-A\varepsilon_{11}}\right)^m} \quad \text{for} \quad \phi = 1$$

$$N_* = \frac{1}{k\left(\frac{B\varepsilon_{11}-a}{b-B\varepsilon_{11}}\right)^m} \quad \text{for} \quad \phi = 0 \tag{12}$$

$$N_* = \frac{1}{k\left(\frac{C\varepsilon_{11}-a}{b-C\varepsilon_{11}}\right)^m} \quad \text{for} \quad \phi = -1$$

Here *A,B,C,k* and *m* are material constants that may be found from the approximation of experimental data curves in relationship between the amplitude of the maximum principal strain and the number of cycles to failure. The method for determination of these material constants based on the multipoint approximation concept is discussed in details in [34].

On the other hand, we can use Eqs (2), (3), (6) and (11) to show analogous relations in these basic experiments.

Considering loading with the strain ratio $\phi=1$ we obtain from Eqs (2), (3), (6) and (11)

$$N_* = \frac{1}{k\left[\frac{\varepsilon_{11}\left(\frac{2}{3}\lambda_1+2\gamma\lambda_3\right)-a}{b-\varepsilon_{11}\left(\frac{2}{3}\lambda_1+2\gamma\lambda_3\right)}\right]^m} \tag{13}$$

Similarly, the relation in the case of loading with the strain ratio $\phi=0$ is

$$N_* = \frac{1}{k\left[\frac{\varepsilon_{11}\left(\frac{2}{3}\lambda_1+\alpha\lambda_2+\gamma\lambda_3\right)-a}{b-\varepsilon_{11}\left(\frac{2}{3}\lambda_1+\alpha\lambda_2+\gamma\lambda_3\right)}\right]^m} \tag{14}$$

In the case of loading with the strain ratio $\phi=-1$, it is not difficult to obtain from Eqs (2), (3), (6) and (11) the following relation

$$N_* = \frac{1}{k\left[\frac{\varepsilon_{11}\left(\frac{2\sqrt{3}}{3}\lambda_1+\alpha\lambda_2\right)-a}{b-\varepsilon_{11}\left(\frac{2\sqrt{3}}{3}\lambda_1+\alpha\lambda_2\right)}\right]^m} \tag{15}$$

Comparing formulas of Eq. (12) with Eqs (13)- (15), respectively, we obtain

$$A = \frac{2}{3}\lambda_1 + 2\gamma\lambda_3$$
$$B = \frac{2}{3}\lambda_1 + \alpha\lambda_2 + \gamma\lambda_3 \qquad (16)$$
$$C = \frac{2\sqrt{3}}{3}\lambda_1 + \alpha\lambda_2$$

Now it is not difficult to find material parameters

$$\lambda_1 = \frac{3}{2\sqrt{3}-1}\left(C + \frac{1}{2}A - B\right)$$
$$\gamma\lambda_3 = \frac{1}{2}A - \frac{1}{3}\lambda_1 \qquad (17)$$
$$\alpha\lambda_2 = C - \frac{2\sqrt{3}}{3}\lambda_1$$

4 Particular cases

Using Eq.(17), we analyze certain possible particular cases, resulting from Eqs (2), (3), (6) and (11), and containing a smaller number of material parameters.

(I) If the results from a set of basic experiments show that

$$A = B, \quad C = \sqrt{3}A \qquad (18)$$

then together with Eq.(17) we obtain

$$\lambda_1 = \frac{3}{2}A, \quad \alpha = \gamma = 0 \qquad (19)$$

Making use of Eq.(19) we can rewrite the equivalent strain given by expression (3) as

$$\varepsilon_e = \frac{3}{2}A\varepsilon_i \qquad (20)$$

Thus, in the case under consideration the equivalent strain includes with the accuracy of the material parameter the stress intensity. The conditions given by Eq.(18) are recommendations for using expression (20) for the equivalent strain in the fatigue damage evolution equation. Non-existence of even one of the equalities in Eq. (18) shows the impossibility of using Eq.(20).

(II) We now assume that from a set of basic experiments, we obtain

$$A \neq B, \quad C = A\left(\sqrt{3}-1\right) + B \qquad (21)$$

Substituting Eq.(21) into Eq.(17), we arrive at the following relation

$$\gamma = 0 \qquad (22)$$

Therefore, the equivalent strain given by Eq.(3) has the following structure

$$\varepsilon_e = \lambda_1\varepsilon_i + \alpha\lambda_2\varepsilon_{11} \qquad (23)$$

Thus, in this case the expression for the equivalent strain in the fatigue damage evolution equation contains only the strain intensity and the maximum principal strain for amplitudes.

(III) We assume the following data are obtained from a set of basic experiments

$$A \neq B, \quad C = \sqrt{3}(2B - A) \qquad (24)$$

Using then Eq.(17) together with Eq.(24) we arrive at the following relation

$$\alpha = 0 \qquad (25)$$

Equivalent strain given by Eq.(3) can now be rewritten as follows:

$$\varepsilon_e = \lambda_1\varepsilon_i + \gamma\lambda_3\varepsilon_0 \qquad (26)$$

Thus, in the case under consideration the expression for the equivalent strain in the fatigue damage evolution equation contains the strain intensity and the volume strain for amplitudes.

(IV) If a set of basic experiments yields

$$A \neq B, \quad C \neq A\left(\sqrt{3}-1\right) + B, \; C \neq \sqrt{3}(2B - A) \qquad (27)$$

we have the most general case of material behavior during low cycle fatigue. The equivalent strain is defined by expression (3) where the appropriate material parameters may be found from Eq.(17).

5 Comparison of theoretical and experimental results

The material tested was the type SUS304 stainless steel at 923K. The detailed description of chemical composition, heat treatment and experimental procedure can be found in [20,21].

First of all we determine the material parameters in the proposed expression (3) for the

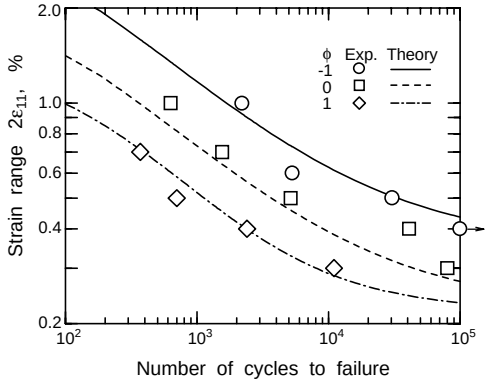

Fig.2. Relationship between maximum strain and fatigue life in basic

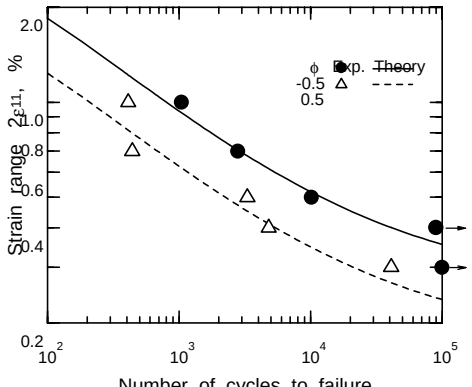

Fig.3. Relationship between maximum strain and fatigue life in model predictions

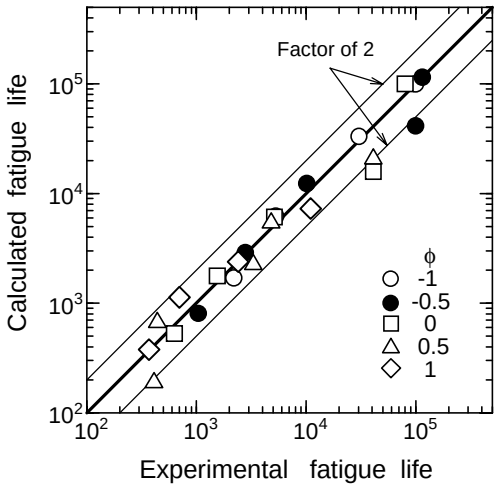

Fig.4. Comparison of experimental and calculated fatigue lives

equivalent strain. Figure 2 shows a comparison of experimentally observed lives of cruciform specimens for basic experiments with the analogous values calculated on the basis of Eq. (12) with the material constants taken as:

$$\mathrm{m} = 1.8830,\ \mathrm{k} = 0.018700,\ \mathrm{a} = 1,\ \mathrm{b} = 14.380$$
$$\mathrm{A} = 1284.47, \mathrm{B} = 801.54, \mathrm{C} = 569.66 \quad (28)$$

Then using Eqs (17) and (28) we obtain the following values of the material parameters:

$$\lambda_1 = 499.60\ ,\gamma\lambda_3 = 475.70\ ,\alpha\lambda_2 = -7.230 \quad (29)$$

Now we can demonstrate a comparison of model predictions on the basis of Eqs (2), (3), (6), (11) and (29) with the experimentally observed fatigue lives of cruciform specimens of the type SUS304 stainless steel for the other levels of the principal strain ratio. This comparison is given in Fig.3. It is seen that the theoretical and experimental results are in satisfactory agreement. Table 1 shows a summary of the model and experimental results. The calculated and experimentally observed fatigue lives can be found in Table, and their graphical form is presented in Fig.4. It is seen that majority of the model results are inside of the scatter band of a factor of 2.

We can integrate Eq.(1) and obtain the following expression for the fatigue damage variable as a function of the number of cycles

$$\omega = 1 - \left[1 - Nk\chi\left(\varepsilon_e\right)\right]^{\frac{1}{k}} \quad (30)$$

Figures 5(a-e) illustrate the results of calculations of the fatigue damage growth in the type SUS304 stainless steel for various maximum principal strains and strain ratios obtained on the basis of Eqs. (2), (3), (11), (29) and (30). It is seen the features of the influence of the maximum strain as well as the strain ratio on the fatigue damage evolution. Note that a law of the fatigue damage growth in Figs 5(a-e) is similar to the evolution law for microcrack density experimentally observed in the 316L stainless steel [35].

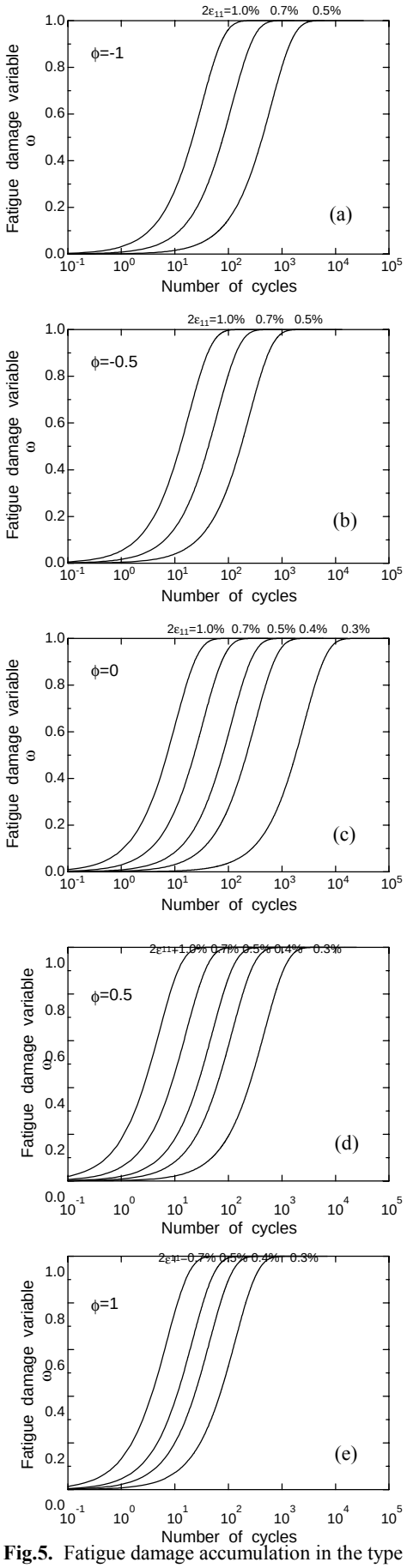

Fig.5. Fatigue damage accumulation in the type SUS304 stainless steel.

6 Conclusion

A new model of continuum damage mechanics associated with the equivalent strain concept has been proposed to describe the fatigue damage evolution in polycrystalline materials under biaxial loading conditions. The proposed expression for the equivalent strain has a general form and includes as particular cases a number of special expressions with a smaller number of material parameters and invariants. Basic experiments for determination of the material parameters in the proposed model have been formulated. Experimentally observed fatigue lives of cruciform specimens for other levels of the principal strain ratios have been compared with the corresponding theoretical values. Experimental data for steel and theoretical results are in satisfactory agreement. Condition of absence of the strain in the normal direction to the specimen surface can be used in the fatigue damage model outlined in this paper.

References

1. **Fatemi A, Yang L** (1998) Cumulative fatigue damage and life prediction theories: a survey of the state of the art for homogeneous materials. Int. J. Fatigue 20(1): 9-34
2. **Sakane M, Ohnami M, Sawada M** (1987) Fracture modes and low cycle biaxial fatigue life at elevated temperature. Trans. ASME Journal of Engineering Materials and Technology 109: 236-243
3. **Socie D** (1993) Critical plane approaches for multiaxial fatigue damage assessment. In: Advances in Multiaxial Fatigue, ASTM STP 1191 (Eds. McDowell D L, Ellis R). American Society for Testing and Materials, Philadelphia, 7-36
4. **Altenbach H, Zolochevsky A** (1996) A generalized fatigue limit criterion and a unified theory of low-cycle fatigue damage. Fatigue Fract. Engng Mater. Struct. 19: 1207-1219
5. **Zolochevsky A, Obataya Y, Betten J** (2000) Critical plane approach with two families of microcracks for modelling of unilateral fatigue damage. Forschung Ingenieurwes. 66 (In press)
6. **Brown M W, Miller K J** (1973) A theory for fatigue failure under multiaxial stress-strain conditions. Proc. Inst. Mech. Engineers 187: 745-755
7. **Fernando U S, Brown M W, Miller K J** (1991) Cyclic deformation and fatigue endurance of En15R steel under multiaxial out-of-phase loading. In: Fatigue under Biaxial and Multiaxial Loading, ESIS 10 (Eds. Kussmaul K, McDiarmid D, Socie D). Mechanical Engineering Publications, London, 337-356
8. **Ogata T, Nitta A, Kuwabara K** (1991) Biaxial low-cycle fatigue failure of type 304 stainless steel under in-phase and out-of-phase straining conditions. In: Fatigue under Biaxial and Multiaxial Loading, ESIS 10 (Eds. Kussmaul K, McDiarmid D, Socie D). Mechanical Engineering Publications, London, 377-392
9. **Xia Z, Kujawski D, Ellyin F** (1996) Effect of mean stress and ratcheting strain on fatigue life of steel. Int. J. Fatigue 18**:** 335-341
10. **Zouani A, Bui-Quoc T, Bernard M** (1999) Fatigue life parameter for type 304 stainless steel under biaxial-tensile loading at elevated temperature. Trans. ASME Journal of Engineering Materials and Technology 121: 305-312.
11. **Łagoda T, Macha E, Będkowski W** (1999) A critical plane approach based on energy concepts: application to biaxial random tension-compression high-cycle fatigue regime. Int. J. Fatigue 21(5): 431-443
12. **Bérard J Y, McDowell D L , Antolovich S D** (1993) Damage observation of a low-carbon steel under tension-torsion low-cycle fatigue. In: Advances in Multiaxial Fatigue, ASTM STP 1191 (Eds. McDowell D L, Ellis R). American Society for Testing and Materials, Philadelphia, 326-344
13. **Weiss J, Pineau A** (1993) Continuous and sequential multiaxial low-cycle fatigue damage in 316 stainless steel. In: Advances in Multiaxial Fatigue, ASTM STP 1191 (Eds. McDowell D L, Ellis R). American Society for Testing and Materials, Philadelphia, 183-203
14. **Robillard M, Cailletaud G** (1991) 'Directionally defined damage' in multiaxial low-cycle fatigue: experimental evidence and tentative modelling. In: Fatigue under Biaxial and Multiaxial Loading, ESIS 10 (Eds. Kussmaul K, McDiarmid D, Socie D). Mechanical Engineering Publications, London, 103-130
15. **Yoshida F, Obataya Y, Shiratori E** (1984) Mechanical ratcheting behaviors of a steel pipe under combined cyclic axial load and internal pressure. In: Proceeding of the Twentyseventh Japan Congress of Materials Research. The Society of Materials Science, Kyoto, 19-23
16. **McDiarmid D L** (1991) Mean stress effects in biaxial fatigue where the stresses are out-of-phase and at different frequencies. In: Fatigue under Biaxial and Multiaxial Loading, ESIS 10 (Eds. Kussmaul K, McDiarmid D, Socie D). Mechanical Engineering Publications, London, 321-335
17. **Ellyin F, Wolodko J D** (1997) Testing facilities for multiaxial loading of tubular specimens. In: Proceedings of the 1995 Symposium on Multiaxial Fatigue and Deformation Testing Techniques, SAE STP 1280. Denver, 7-24
18. **Sakane M, Ohnami M** (1991) Creep-fatigue in biaxial stress states using cruciform specimen. In: Fatigue under Biaxial and Multiaxial Loading, ESIS 10 (Eds. Kussmaul K, McDiarmid D, Socie D). Mechanical Engineering Publications, London, 265-278
19. **Nurtjahjo A, Ott W, Marissen R, Trautmann K-H, Nowack H** (1992) Comparison of the prediction capability of crack initiation life prediction methods for biaxial loading conditions. In: Low Cycle Fatigue and Elasto-Plastic Behaviour of Materials-3 (Ed. Rie K-T). Elsevier, London, 317-324
20. **Itoh T, Sakane M, Ohnami M, Takahashi Y, Ogata T** (1992) Nonproportional multiaxial low cycle fatigue using cruciform specimen at elevated temperature. In: Creep: Characterization, Damage and Life Assessment, Proceedings of the Fifth International Conference on Creep of Materials (Eds. Woodford D A, Townley C H A, Ohnami M). ASM International, Materials Park, 331-339
21. **Itoh T, Sakane M, Ohnami M** (1994) High temperature multiaxial low cycle fatigue of cruciform specimen. Trans. ASME Journal of Engineering Materials and Technology 116: 90-98
22. **Ogata T, Takahashi Y** (1999) Development of a high-temperature biaxial fatigue testing machine using a cruciform specimen. In: Multiaxial Fatigue and

Fracture, ESIS 25 (Eds. Macha E, Będkowski W, Łagoda T). Elsevier, Amsterdam, 101-114
23. **Sakane M, Ohnami M, Hamada N** (1988) Biaxial low cycle fatigue for notched, cracked, and smooth speciemens at high temperatures. Trans. ASME Journal of Engineering Materials and Technology 110: 48-54
24. **Tschegg E K, Mayer H R, Czegley M, Stanzl S E** (1991) Influence of a constant mode III load on Mode I fatigue crack growth thresholds. In: Fatigue under Biaxial and Multiaxial Loading, ESIS 10 (Eds. Kussmaul K, McDiarmid D, Socie D). Mechanical Engineering Publications, London, 213-222
25. **Kachanov L M** (1958) On the time to failure under creep conditions. Izv. AN SSSR Otd. Tekhn. Nauk (8): 26-31
26. **Rabotnov Yu N** (1959) On the mechanism of long-term failure. In: Problems of Strength for Materials and Structures. AN SSSR, Moscow, 5-7
27. **Kachanov L M** (1986) Introduction to Continuum Damage Mechanics. Martinus Nijhoff, Dordrecht
28. **Rabotnov Yu N** (1969) Creep Problems in Structural Members. North-Holland, Amsterdam
29. **Lemaitre J, Chaboche J L** (1990) Mechanics of Solid Materials. Cambridge University Press, Cambridge
30. **Lemaitre J** (1992) A Course on Damage Mechanics. Springer-Verlag, Berlin
31. **Betten J** (1993) Kontinuumsmechanik. Springer-Verlag, Berlin
32. **Altenbach H, Altenbach J, Zolochevsky A** (1995) Erweiterte Deformationsmodelle und Versagenskriterien der Werkstoffmechanik. Deutscher Verlag für Grundstoffindustrie, Stuttgart
33. **Krajcinovic** D (1996) Damage Mechanics. Elsevier, Amsterdam
34. **Yoshida F, Urabe M, Toropov V V** (1998) Identification of material parameters in constitutive model for sheet metals from cyclic bending tests. Int. J. Mech. Science 40: 237-249
35. **Bataille A, Magnin T** (1994) Surface damage accumulation in low-cycle fatigue: physical analysis and numerical modelling. Acta Metall. Mater. 42(11): 3817-3825

Table 1. Summary of the theoretical and experimental results for the type SUS304 stainless steel at 923K

ϕ	$2\varepsilon_{11}$ (%)	n_1	n_2	n_3	m_1	m_2	m_3	ε_e	N_*	
									Exp.	Theory
1.0	0.7	-	-	-	$1/\sqrt{2}$	$1/\sqrt{2}$	0	4.4872	370	377
	0.5	-	-	-	$1/\sqrt{2}$	$1/\sqrt{2}$	0	3.4051	700	1131
	0.4	-	-	-	$1/\sqrt{2}$	$1/\sqrt{2}$	0	2.5641	2400	2392
	0.3	-	-	-	$1/\sqrt{2}$	$1/\sqrt{2}$	0	1.9231	11000	7285
0.5	1.0	1	0	0	$1/\sqrt{2}$	$1/\sqrt{2}$	0	4.9751	410	189
	0.7	1	0	0	$1/\sqrt{2}$	$1/\sqrt{2}$	0	3.4825	440	669
	0.5	1	0	0	$1/\sqrt{2}$	$1/\sqrt{2}$	0	2.4875	3300	2248
	0.4	1	0	0	$1/\sqrt{2}$	$1/\sqrt{2}$	0	1.9900	4800	5414
	0.3	1	0	0	$1/\sqrt{2}$	$1/\sqrt{2}$	0	1.4925	41000	20702
0.0	1.0	1	0	0	$1/\sqrt{2}$	$1/\sqrt{2}$	0	4.0000	630	530
	0.7	1	0	0	$1/\sqrt{2}$	$1/\sqrt{2}$	0	2.8000	1550	1772
	0.5	1	0	0	$1/\sqrt{2}$	$1/\sqrt{2}$	0	2.0000	5150	6097
	0.4	1	0	0	$1/\sqrt{2}$	$1/\sqrt{2}$	0	1.6000	41000	15875
	0.3	1	0	0	$1/\sqrt{2}$	$1/\sqrt{2}$	0	1.2000	80000	>100000
-0.5	1.0	1	0	0	$1/\sqrt{2}$	$1/\sqrt{2}$	0	3.3557	1040	803
	0.7	1	0	0	$1/\sqrt{2}$	$1/\sqrt{2}$	0	2.3490	2800	2888
	0.5	1	0	0	$1/\sqrt{2}$	$1/\sqrt{2}$	0	1.6778	10150	12318
	0.4	1	0	0	$1/\sqrt{2}$	$1/\sqrt{2}$	0	1.3423	>100000	41318
	0.3	1	0	0	$1/\sqrt{2}$	$1/\sqrt{2}$	0	1.0067	>100000	>100000
-1.0	1.0	1	0	0	$1/\sqrt{2}$	$1/\sqrt{2}$	0	2.8490	2200	1701
	0.7	1	0	0	$1/\sqrt{2}$	$1/\sqrt{2}$	0	1.9943	5300	6217
	0.5	1	0	0	$1/\sqrt{2}$	$1/\sqrt{2}$	0	1.4245	30500	33121
	0.3	1	0	0	$1/\sqrt{2}$	$1/\sqrt{2}$	0	0.8547	>100000	>100000